Journal of Chemical Reviews

2026, Volume 8, Issue 2

Review Article

Electroactive Clay Polymer Nanocomposites for Sustainable Device Applications

R.M.G. Rajapakse[1,*], Theekshana Malalagama[2], Yasas Bandara[1], Ho Soon Min[3]

[1]*Department of Chemistry, University of Peradeniya, Peradeniya 20400, Sri Lanka*
[2]*National Engineering Research Center of Industrial Wastewater Detoxication and Resource Recovery, Research Center for Eco-Environmental Sciences, Chinese Academy of Sciences, Beijing 100085, China*
[3]*Faculty of Health and Life Sciences, INTI International University, Putra Nilai, 71800, Negeri Sembilan, Malaysia*

Use your device to scan and read the article online

Citation: R.M.G. Rajapakse, T. Malalagama, V.M.Y.S.U. Bandara, H. Soonmin, **Electroactive Clay Polymer Nanocomposites for Sustainable Device Applications**. *J. Chem. Rev.*, **2026,** *8*(2), 214-240.

https://doi.org/10.48309/JCR.2026.537691.1488

ARTICLE INFO

Received: 2025-07-30
Revised: 2025-09-09
Accepted: 2025-10-01
ID: JCR-2507-1488

Keywords:
Clay–conducting polymer nanocomposites, Montmorillonite, Electronically conducting polymers, *In situ* oxidative polymerisation, water pollution, wastewater treatment

ABSTRACT

Clay–conducting polymer nanocomposites (CPNs) have gained attention as versatile materials that are easy to produce and useful across a wide range of technologies. Combinations of montmorillonite (MMT) clay with electronically conducting polymers (ECPs) such as polyaniline (PANI), polypyrrole (PPY), and poly(ethylenedioxythiophene) (PEDOT) stand out. These materials combine mechanical strength with the ability to conduct electricity, making them multifunctional. This review explores the development of MMT–ECP nanocomposites from early electroactive films to their growing roles in sustainable energy, industrial waste management, environmental cleanup, wastewater treatment, biomedical devices, and smart packaging. Different methods used to make these materials, such as *in situ* oxidative polymerization, solution intercalation, and electrochemical deposition are discussed. Each method influences how well the clay layers separate, how the polymer spreads, and how strongly the components bond together. Additionally, the effect of the structure of these nanocomposites on their performance is assessed, using tools such as spectroscopy, microscopy, electrochemistry, and thermal analysis. Their applications in areas including supercapacitors, solid-state batteries, electromagnetic interference (EMI) shielding, chemical sensors, and water purification are reviewed, with special attention to eco-friendly processes and systems that can integrate with biological environments. The review emphasizes strategies aimed at meeting performance needs without compromising sustainability. Cross-sectoral relevance is highlighted, spanning well-established areas such as energy storage alongside emerging fields such as biomedical systems and smart packaging. By bringing together insights from materials science, nanotechnology, and electrochemistry, these nanocomposites offer a promising foundation for building the green technologies of the future.

***Corresponding Author: R.M.G. Rajapakse** (rmgr@sci.pdn.ac.lk)*

R. M. G. Rajapakse: He is a Senior Professor of Chemistry at the University of Peradeniya, Sri Lanka. He obtained his Ph.D. and D.I.C. from Imperial College London and completed postdoctoral research in photoelectrochemistry under Professor W. John Albery. His research focuses on nanomaterials and nanocomposites for energy conversion, water purification, and environmental remediation. Professor Rajapakse has held visiting and research appointments at the Max Planck Institute for Polymer Research (Germany), Shizuoka University (Japan), Western Norway University of Applied Sciences, the Research Centre for Eco-Environmental Sciences (RCEES) of the Chinese Academy of Sciences, and several universities in the United Kingdom and the United States. He is a Fellow of the Royal Society of Chemistry (UK) and the National Academy of Sciences of Sri Lanka, and a member of the American Association for the Advancement of Science (AAAS), Sri Lanka Association for the Advancement of Science (SLAAS), and the Institute of Chemistry, Ceylon. He has supervised over 50 M.Phil./Ph.D. candidates, published more than 150 indexed papers (h-index 38), and held four patents. His work has earned national recognition, including the CVCD, Presidential, and NSF SUSRED Awards.

Theekshana Malalagama: She is recognized for her contributions to sustainable water treatment, particularly in electrochemical processes such as electrodialysis for rural and resource-limited communities. With a Ph.D. in Environmental Engineering, she has led extensive field and laboratory investigations addressing groundwater contamination in Sri Lanka. Her research integrates membrane technology, renewable energy, and community-based water management. She has published in high-impact peer-reviewed journals and is actively engaged in international collaborations across Sri Lanka and China. Her current focus includes low-cost decentralized desalination systems, membrane fouling control, and developing resilient water supply solutions for climate-vulnerable regions.

Yasas Bandara: He assists in graduate and undergraduate research, integrating renewable energy and membrane technology. His work includes projects on zinc/bromine gel batteries, membrane development, solar cells, and electrochemical studies of mahanimbine isolated compounds. He contributes to advancing sustainable energy solutions and electrochemical applications within environmental and energy engineering contexts.

Ho Soon Min is internationally recognized for his contributions to green chemistry, semiconductor materials, activated carbon, thin film solar cells, and renewable energy. He earned his Ph.D. degree in Materials Chemistry from Universiti Putra Malaysia and currently serves at INTI International University, Malaysia. He has published over 170 indexed papers, 45 book chapters, and 3 books. He has received multiple international awards and serves as a reviewer for over 650 manuscripts, editor for 30 journals, and board member for 85 journals. His global collaborations span Asia and beyond, and he plays a leading role in advancing sustainable materials research and education.

Content

1. Introduction

Nanocomposites are materials that contain at least one phase with dimensions at the nanoscale. They combine the properties of their individual constituents in ways that can be either subtle or highly significant, often resulting in novel mechanical, electrical, thermal, and optical characteristics that cannot be achieved by the components alone. These systems encompass a wide variety of combinations-for example, polymers and amorphous materials integrated with other components of differing properties, all typically within dimensions below 100 nm. In developing nanocomposite materials, fillers such as inorganic nanoparticles, carbon nanotubes, or clay play a crucial role in reinforcing and modifying the properties of the polymer matrix [1]. Clay–polymer nanocomposites (CPNs) have drawn considerable attention over the past three decades as hybrid materials that combine and enhance the individual strengths of their components. They improve the processability and functionality of polymers while retaining the dimensional stability and large surface area typically found in layered silicates. These nanocomposites benefit from the ability of nano-clay minerals, especially smectites like montmorillonite (MMT) to intercalate or exfoliate within polymer matrices. This results in enhanced thermal, mechanical, electrical, and barrier properties, even at relatively low clay contents. Because of these advantages, CPNs are increasingly used in energy storage, electronics, catalysis, packaging, and biomedical applications [2-4]. Among the various layered silicates, MMT stands out as the most widely studied, thanks to its high aspect ratio, excellent cation exchange capacity, and ease of chemical modification, which enables compatibility with both hydrophilic and hydrophobic polymers [5]. The internal structure of the nanocomposite, whether it's intercalated, exfoliated, or tactoid, plays a key role in determining how much its properties are improved. Popular synthesis methods such as *in situ* oxidative polymerisation, melt intercalation, and solution blending are widely employed to ensure even dispersion of clay layers and strong bonding between components [2]. The foundational

study by Okada and Usuki on nylon-6/MMT systems [6] demonstrated how effectively nanoclays can reinforce polymer matrices, sparking a surge in research on similar polymer–clay systems. Within this growing body of work, Rajapakse *et al.* have made notable contributions to synthesizing, characterizing, and applying conducting clay-polymer nanocomposites. For example, Wijeratne *et al.* [7] found that MMT–polyaniline nanocomposites exhibited improved thermal stability, while Rajapakse *et al.* [8] synthesized PEDOT–MMT nanocomposites using *in situ* oxidative polymerization, showing significant improvements in both electrical conductivity and thermal properties. Moreover, Rajapakse *et al.* demonstrated that polypyrrole–MMT nanocomposites are promising cathode materials for oxygen reduction reactions in electrochemical systems [9]. MMT is a layered aluminosilicate clay mineral with a permanent negative charge. This charge results from isomorphic substitutions—mainly Al^{3+} replacing Si^{4+} in tetrahedral layers and Mg^{2+} replacing Al^{3+} in octahedral sheets. These negative charges are balanced by hydrated, exchangeable cations such as Na^{+} and Ca^{2+}, located in the interlayer galleries. MMT's high cation exchange capacity (around 100 meq g^{-1}) enables the insertion of positively charged conducting polymer chains, such as the emeraldine salt form of $PANI^{+}$, during *in situ* oxidative polymerization in aqueous dispersions [10]. **Figure 1**(a) shows the structure of an intercalated MMT–PANI nanocomposite, where positively charged $PANI^{+}$ chains are inserted between the negatively charged layers of MMT. This process displaces smaller hydrated counterions like $Na^{+}{\cdot}nH_2O$, leading to a substantial increase in the interlayer (basal) spacing. The earlier studies reported that dry pristine Na^{+}–MMT shows a basal spacing (d_{001}) of roughly 9 Å. Upon hydration, this expands by about 3 Å per water monolayer linked with interlayer cations. In contrast, X-ray diffraction (XRD) analysis of MMT–PANI nanocomposites dried at 150 °C for 2 h showed an expanded spacing of approximately 24 Å, confirming the successful incorporation of bulky PANI chains and radical cations within the clay structure [11]. As the amount of PANI increases, the electrostatic and van der Waals forces holding adjacent clay layers together are gradually weakened. When the polymer loading exceeds a critical level, the clay layers fully delaminate and separate into individual nanosheets. This leads to an exfoliated MMT–PANI structure, illustrated in **Figure 1**(b), where the silicate layers are evenly distributed throughout the PANI matrix. These exfoliated forms offer better mechanical strength, enhanced thermal and gas barrier properties, and stronger interfacial bonding between the polymer and the clay.

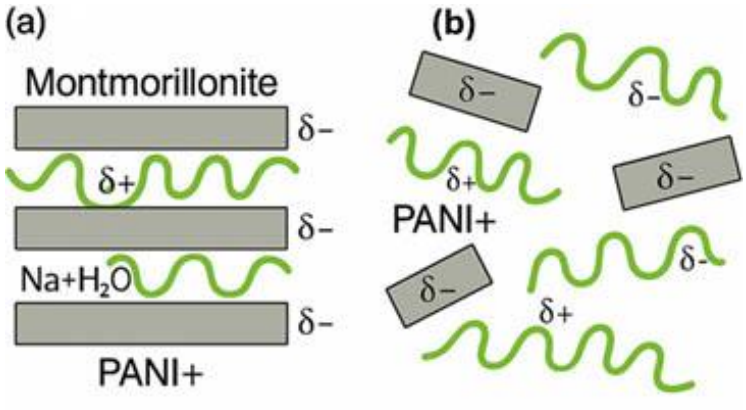

Figure 1. Schematic of (a) intercalated and (b) exfoliated MMT–PANI nanocomposites. (a) $PANI^{+}$ chains intercalate between MMT layers, expanding spacing to ~24 Å. (b) At higher polymer loadings, silicate layers fully delaminate and disperse, forming an exfoliated nanostructure with enhanced interactions and properties

Beyond improvements in thermal and electrical performance, these nanocomposites show promise across a variety of applications. For instance, adding MMT to polyethylene oxide (PEO) matrices enhances ionic conductivity in solid polymer electrolytes [10,11]. Krishantha *et al.* [11] developed Cu^{+}-conducting MMT–polypyrrole composites that display mixed ion-electron conductivity, making them useful in sensors and redox capacitors. Other studies on polypyrrole–Fuller's Earth [12] and polyaniline–MMT nanocomposites [13] reported higher conductivity, redox activity, and improved environmental stability. Rajapakse's team also explored eco-friendly synthesis of polyaniline using copper (II) scorpionate catalysts, producing high-quality materials with lower environmental impact [14]. These green synthesis methods align with the growing demand for sustainable nanomaterials. Additionally, their work on PEDOT-functionalized phosphine ligands coordinated with Pd (II) and Pt (II) complexes demonstrated the integration of organometallic and polymer chemistry for advanced optoelectronic applications [15]. On a broader scale, CPNs are finding new roles across multiple sectors. In electronics, they are used for electromagnetic interference (EMI) shielding, flexible circuits, and antistatic coatings [16,17]. In energy storage, they serve as electrodes, cathodes, and solid electrolytes in batteries and supercapacitors [18-20]. Their excellent barrier properties, especially when exfoliated, make them ideal for food and pharmaceutical packaging [21]. In the biomedical field, their biocompatibility supports applications in drug delivery and tissue engineering [22,23]. Environmental uses include removal of pollutants, heavy metals, and dyes, leveraging the high surface area and chemical tunability of clay surfaces [9,13,24]. The field of clay–polymer nanocomposites continue to evolve rapidly, with an increasing focus on bio-based polymers, green production methods, and multifunctional designs. The wide-ranging contributions by Rajapakse *et al.* underscore the potential of these materials to balance high performance with sustainability. Recent developments in conducting polymers (CPs) have also broadened their biomedical applications, especially when engineered for biodegradability and biological activity. Polypyrrole (PPy) stands out among CPs for its excellent conductivity, straightforward synthesis, and ability to incorporate bioactive dopants, making it ideal for interaction with biological systems. Ateh *et al.* [25] emphasized PPy's compatibility with biomolecules, allowing its use in biosensors and as a conductive platform for cell growth and tissue engineering. More recently, work by Kenry and Liu [26] has focused on biodegradable CPs that combine electronic function with safe degradation pathways. These materials hold great promise for use in neural interfaces, temporary implants, and drug delivery systems [12,18]. Researchers are designing these polymers to support cell adhesion, growth, and differentiation while also providing electrical cues to aid tissue regeneration. Incorporating nanostructured components or biocompatible fillers such as clays, hydrogels, or bioceramics, further boosts their electrochemical performance, mechanical strength, and biodegradability. This opens up exciting new possibilities in regenerative medicine and soft bioelectronics [27,29]. This review critically examines recent progress, highlighting advances in synthesis techniques, structure–property relationships, and the growing range of applications in energy, electronics, environmental, and biomedical technologies.

2. Synthesis Strategies

The way MMT–ECP nanocomposites are synthesized plays a key role in shaping their final structure, appearance, and performance. Researchers have developed several techniques to incorporate conducting polymers into the interlayer spaces or onto the surfaces of montmorillonite, aiming for even dispersion, strong bonding at the interface, and high conductivity. The three most common synthesis methods are *in situ* oxidative polymerization, solution blending for intercalation, and electrochemical polymerization. Among these, *in situ* oxidative polymerization is the most

widely used. This method involves polymerizing monomers like aniline, pyrrole, or EDOT in the presence of an oxidizing agent (*e.g.,* ammonium persulfate or $FeCl_3$) and either intercalated or exfoliated clay particles. It promotes close contact between the polymer chains and clay surfaces, improving both the electrical connectivity and the overall structural strength of the material. For example, Rajapakse and his team observed notable improvements in the thermal and electrical behavior of MMT–polyaniline and MMT–PEDOT composites made using this technique [9]. In solution intercalation, clay is typically dispersed in polar solvents such as water, ethanol, or methanol for hydrophilic systems [30], while polar aprotic solvents such as *N*,*N*-dimethylformamide (DMF), dimethyl sulfoxide (DMSO), or tetrahydrofuran (THF) are used when incorporating hydrophobic polymers or organo-modified clays [31]. The polymer solution or monomer is then introduced to facilitate intercalation into the clay galleries. The polymer chains gradually migrate into the clay's interlayer spaces, forming either intercalated or partially exfoliated structures. This method is useful for processing at low temperatures and offers better control over the ratio of polymer to clay. However, unless it is followed by additional functionalization or heat treatment, the bonding at the interface may be weaker [32]. Electrochemical polymerization has become more popular for producing thin films of MMT–ECP nanocomposites directly on conductive surfaces. In this method, the monomer is oxidized electrochemically in the presence of suspended or fixed clay particles. One major benefit of this approach is the ability to fine-tune the film's thickness, shape, and doping level by adjusting the voltage and duration of the deposition. Rajapakse and his team have used this technique to develop clay–PPy electrodes with better redox behavior and improved stability in different environments [9,33]. Newer methods are also gaining attention. These include melt intercalation [34], where the polymer is blended with MMT at high temperatures without using any solvents, and green synthesis routes that rely on bio-based oxidants [35], water-based systems [36], or one-pot synthesis [37] techniques. Such approaches are increasingly important in the push toward sustainable materials and hold promise for commercial-scale production.

3. Materials and Experimental Procedures

3.1. Reagents and materials

Researchers typically used aniline (≥99%), pyrrole (98%), 3,4-ethylenedioxythiophene (EDOT, 97%), ammonium persulfate (APS), ferric chloride ($FeCl_3$), sodium dodecyl sulphate (SDS), hydrochloric acid (HCl), sulphuric acid (H_2SO_4), and sodium montmorillonite (Na^+-MMT, CEC ≈ 92 meq/100 g). These chemicals were generally sourced from Sigma-Aldrich and used as received, without further purification [12,38]. Deionised water with a resistivity of ≥18.2 MΩ·cm was used throughout all experimental steps.

3.2. Clay pre-treatment and exfoliation

Prior to composite preparation, sodium montmorillonite (Na^+–MMT) was purified and activated to enhance its dispersion and intercalation capacity. The raw clay was first acid-treated by dispersing 10 g L^{-1} of Na^+–MMT in 1 M HCl and stirring for 24 h at room temperature. The suspension was then repeatedly washed with deionized water until the filtrate reached neutral pH (≈7), centrifuged at 6,000 rpm for 10 min, and the recovered solid was dried at 80 °C overnight before grinding to a fine powder [39]. For organo-modified clays, cation exchange was performed by stirring a 1 wt% clay dispersion in 0.1 M cetyltrimethylammonium bromide (CTAB) solution for 12 h at 50 °C, followed by washing to remove free surfactant and drying under vacuum. Exfoliation of the clay layers was achieved by preparing a 1 wt% aqueous suspension and subjecting it to probe ultrasonication at 400 W, 20 kHz for 60 min in an ice bath to avoid overheating. The resulting dispersion was further stabilized by mechanical stirring for 24 h [40]. This treatment yielded

highly dispersed montmorillonite platelets with enlarged basal spacing, suitable for subsequent polymer intercalation and composite synthesis.

3.3. In situ oxidative polymerization

PANI–MMT nanocomposites were commonly synthesized using *in situ* oxidative polymerization. In a typical process, aniline (0.1 M) was dissolved in 1 M HCl and added to a pre-sonicated 1 wt% MMT dispersion. The mixture was maintained at 0–5 °C under constant stirring at 300 rpm. An aqueous solution of ammonium peroxydisulfate (APS) (with an APS: aniline molar ratio of 1.25:1) was then added dropwise as the oxidant. Polymerization proceeded for 6–12 hours. The resulting dark-green precipitate was collected by filtration, washed three times with 100 mL deionized water until the filtrate reached neutral pH, followed by two rinses with ethanol (50 mL each), and finally dried under vacuum at 60 °C for 12 h [12,13,38-40]. For PPy–MMT composites, pyrrole monomer was dispersed in an aqueous solution containing 1 wt% MMT and 5 mM SDS as dispersant. Oxidative polymerization was started by the slow addition of $FeCl_3$ (with a $FeCl_3$: pyrrole molar ratio of 2:1) at room temperature. The black precipitate that formed was filtered, washed, and dried in a vacuum oven. This method efficiently encouraged the intercalation of PPy chains into the clay layers [12,13,38-41].

In studies involving electroactive films, researchers used electrochemical polymerization in a three-electrode setup, with a platinum working electrode, an Ag/AgCl reference electrode, and a platinum wire as the counter electrode. The electrolyte contained the monomer (either aniline or EDOT), exfoliated MMT (0.5–1 wt%), and a supporting electrolyte such as tetrabutylammonium hexafluorophosphate ($TBAPF_6$) in acetonitrile. Polymer growth was controlled either potentiostatically or through cyclic voltammetry in the range of −0.2 to +1.0 V at a scan rate of 50–100 mV/s. After deposition, the films were rinsed with acetonitrile, dried at room temperature, and stored in a desiccator until further testing [42-44].

4. Analytical Methods

A wide range of analytical and characterization techniques has been used to explore the physicochemical, structural, thermal, morphological, electrical, and electrochemical properties of clay–conducting polymer (CP) nanocomposites. The choice of methods generally depends on the type of polymer (such as polyaniline, polypyrrole, or PEDOT), the clay used (such as Na^+-montmorillonite or organoclays), and the intended end-use (including energy storage, sensors, or barrier films). Fourier-transform infrared (FTIR) spectroscopy is one of the most common techniques used to study the chemical structure and interactions between polymer chains and the clay surface. Changes or shifts in band intensities—particularly in the Si–O stretching (~1,040 cm^{-1}), C–N stretching (~1,300–1,350 cm^{-1}), and N–H bending (~1,500–1,600 cm^{-1}) regions—can signal interfacial bonding or intercalation processes. In this study, the chemical structure and interfacial interactions within the MMT–CP nanocomposite were analyzed using Fourier-transform infrared (FTIR) spectroscopy. As illustrated in **Figure 2**, the spectrum shows characteristic absorption bands such as O–H stretching (~3,500 cm^{-1}), N–H bending (~1,600 cm^{-1}), C–N stretching (~1,350 cm^{-1}), and Si–O stretching (~1,000 cm^{-1}), confirming the hybrid nature of the composite. The simulated FTIR spectrum of the MMT–PANI nanocomposite also displays key vibrations from O–H, C=N, and Si–O groups. When compared with the experimental data (**Table 1**), moderate shifts are observed in notable peaks—such as C–N stretching (~1,400 cm^{-1} in the simulated data versus ~1,300 cm^{-1} experimentally) and quinoid/benzenoid ring vibrations (~1,600 cm^{-1} versus ~1,580 cm^{-1}). These shifts provide strong evidence of the interaction between polyaniline chains and montmorillonite layers, consistent with earlier research findings [45-50].

Table 1. Comparison of simulated and experimental FT-IR bands for MMT–PANI nanocomposite, showing vibrational assignments, wavenumber shifts, and relevant literature references

Wavenumber (cm^{-1})	Assignment	Material	Remarks	Ref.
3620	O–H stretching of structural hydroxyl groups	MMT	Sharp band, associated with inner Al–OH	[46,47]
1,040	Si–O stretching	MMT	Strong and broad, characteristic of phyllosilicates	[46,49]
520	Si–O–Al (or Si–O–Si) bending	MMT	Out-of-plane vibrations of tetrahedral layers	[46,48]
1,570	C=C stretching (quinoid ring)	CP (PANI)	Indicates oxidized segments in PANI	[51,52]
1,490	C=C stretching (benzenoid ring)	CP (PANI)	Indicates reduced segments in PANI	[51,52]
1,300	C–N stretching	CP (PANI)	Typical for secondary aromatic amines	[51,53]
1,140	N=Q=N stretching (quinoid structure)	CP (PANI)	Associated with electronic delocalisation	[52,53]
1,560	C=C (quinoid, shifted)	MMT–CP	Downshift due to hydrogen bonding/clay interaction	[12,51]
1,480	C=C (benzenoid, shifted)	MMT–CP	Slight shift implies altered electronic structure	[12,51]
1,280	C–N (shifted)	MMT–CP	Suggests bonding between clay surface and amine groups	[12,51]
1,145	N=Q=N (slightly shifted)	MMT–CP	Shift due to altered conjugation in the presence of MMT	[12,52]
1,035	Si–O (slightly shifted)	MMT–CP	Indicates retained clay structure but perturbed environment	[12,46, 51]
520	Si–O–Al bending	MMT–CP	Retained from MMT, often with broadened profile	[12,48,51]
~3,420 (broad)	O–H/N–H overlapping stretch	Starch-MMT/PANI	Reduced intensity in composite due to overlap of starch and PANI bands	[54]
3,737	N–H stretching shift	PANI-DSA/MMT	Shift from 3,729 indicates PANI–MMT interaction	[55]
2,917–2,931	Quinoid C–H stretching (shifted)	PANI-DSA/MMT	Composition-dependent shift showing dopant effect	[55]

1,238–1,311	C–N benzenoid stretching (shifted)	PANI-DSA/MMT	Shift increases with MMT content, indicating strong interaction	[55]
1,045–1,124	Quinoid C–H bending overlap with Si–O–Si	PANI-DSA/MMT	Merged bands confirm interfacial coupling	[55]

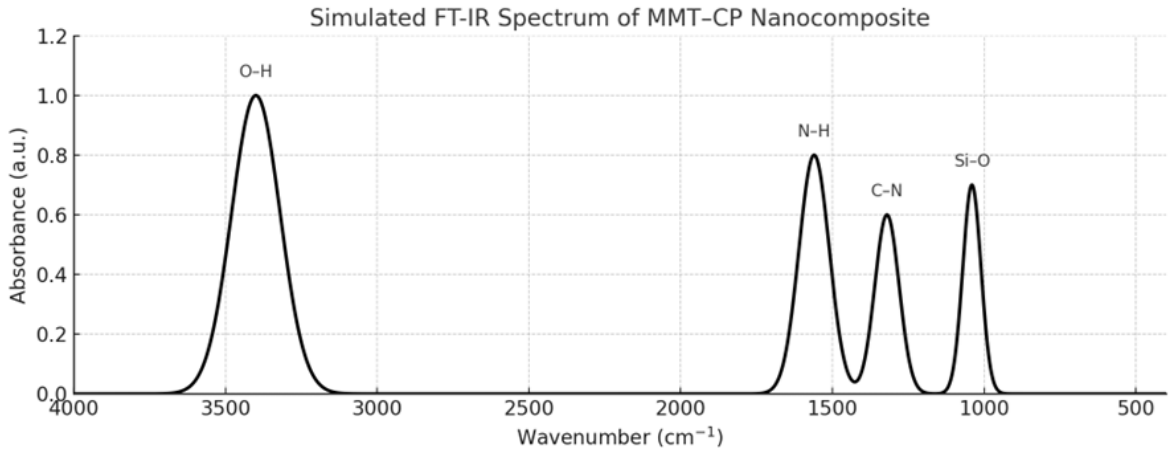

Figure 2. FT-IR spectrum of MMT–CP nanocomposite showing characteristic bands at ~3,500, ~1,600, ~1,350, and ~1,000 cm^{-1}.[46]

X-ray diffraction (XRD) [56] is a key technique used to understand the basal spacing and structural organization of clay layers in nanocomposites. When the (001) reflection shifts to lower 2θ values, it usually signals that the polymer has entered the clay layers (intercalation). Meanwhile, peak broadening or disappearance can suggest that the clay tactoids have separated (exfoliation). These interlayer distances are typically calculated using Bragg's law. The simulated powder X-ray diffraction (p-XRD) patterns for pristine MMT, PANI, and the MMT–PANI nanocomposite display distinct features that reflect their crystalline structures and how they combine in the composite. As shown in **Figure 3**, pristine MMT shows a sharp (001) peak at around 7° 2θ, indicating a regular interlayer distance of about 1.26 nm. In contrast, PANI presents broad signals near 15°, 20°, and 25° 2θ, typical of its semi-crystalline structure and π–π stacking. For the MMT–PANI nanocomposite, the (001) peak shifts to ~4.5° 2θ and becomes significantly broader, with a faint shoulder remaining near 7°, suggesting that PANI chains have successfully intercalated into the clay layers, causing partial exfoliation. A broad hump near 20° also confirms the presence of short-range ordering from the PANI component. These changes in peak positions and widths point to the formation of nanostructured materials with strong polymer–clay interactions. **Table 2** summarizes these observations and links them with structural interpretations and supporting references from existing studies.

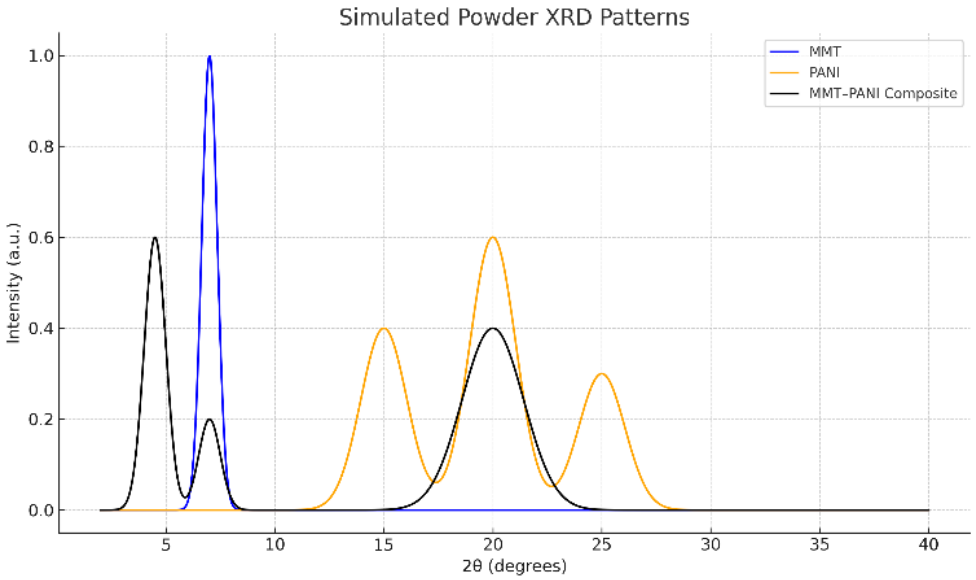

Figure 3. The simulated powder XRD patterns for MMT, PANI, and the MMT–PANI nanocomposite (in blue, orange, and black, respectively)

Table 2. Simulated powder XRD patterns of pristine MMT, polyaniline, and the MMT–PANI nanocomposite

Sample	Key 2θ Peak Positions (°)	Peak Characteristics	Interpretation	Ref.
MMT	~7	Sharp and intense	(001) basal reflection; ordered layered structure with d ≈ 1.26 nm	[57]
PANI	~15, ~20, and ~25	Broad humps	Semi-crystalline; π–π stacking and backbone periodicity	[12]
MMT–PANI	~4.5 (main), ~7 (shoulder), and ~20	Broadened, shifted, with weak shoulder	Intercalated and partially exfoliated structure; increased interlayer spacing (d ≈ 1.96 nm); PANI–clay interaction	[58,59]
PANI–DSA/MMT	~6 (shifted from 7)	Broadened and less intense	Intercalation with gallery expansion (d ≈ 1.48 nm)	[55]
MMT: PANI composites	7 → disappearance	Disappearing basal reflection at high PANI	Transition from intercalated → exfoliated layers	[60]
PANI/MMT/La^{3+}	new low-angle peak	Additional ordering	Lanthanum-assisted intercalation; nanowire network structure	[61]

Thermogravimetric analysis (TGA) and differential scanning calorimetry (DSC) are used to evaluate thermal stability, degradation behavior, and possible interactions between the clay and polymer components. TGA curves usually show multiple weight loss steps that represent the loss of moisture, release of dopants, and eventual breakdown of the polymer backbone. A noticeable improvement in thermal stability often indicates successful integration of clay into the polymer matrix. The thermal properties of the MMT–PANI

nanocomposite were studied using simulated TGA and DSC techniques, as illustrated in **Figure 4**.

The TGA results show three main stages of weight loss: a small drop near 100 °C due to water evaporation, a larger loss around 250 °C linked to dopant breakdown, and a major weight reduction at about 450 °C from the oxidative degradation of the polyaniline backbone. The DSC data support these findings, showing endothermic peaks at ~100 °C and ~250 °C, and an exothermic peak around 450 °C. Notably, no melting point is observed, which aligns with the amorphous-to-semicrystalline nature of polyaniline and the stable thermal profile of montmorillonite [12,47,58,59,62-64]. The simulated TGA and DSC profiles of the MMT–PANI nanocomposite reveal three distinct thermal events corresponding to water loss (~100 °C), dopant loss (~250 °C), and major polymer degradation (~450 °C), which closely aligns with experimentally reported data in the literature (**Table 3**) [12,57]. Scanning electron microscopy (SEM) and transmission electron microscopy (TEM) are used to explore surface texture and nanoscale structural features. TEM is especially useful for confirming whether the clay layers are intercalated or exfoliated by directly showing their separation, while SEM helps identify surface cracks, porosity, or compactness based on the synthesis method and amount of clay used. **Figure 5** shows simulated SEM images comparing pure PANI with its nanocomposite containing montmorillonite, highlighting the changes in texture and morphology after nano-clay is added. SEM images of fractured surfaces usually reveal a smoother texture in the pure polymer, while nanocomposites appear rougher and more layered due to the presence of clay platelets and enhanced stress-transfer regions. Simulated SEM and TEM images of the MMT–PANI nanocomposite reveal common structural features like rough surfaces coated with polymer and partially exfoliated silicate layers distributed throughout the matrix (**Figure 5**). These findings match well with those previously reported in the literature (**Table 4**) [8,53,65]. UV-Vis-NIR spectroscopy is frequently applied to study electronic transitions in conducting polymers and to evaluate doping levels, especially in polyaniline and polypyrrole composites. Shifts in absorption bands correlate with changes in oxidation states or extended conjugation due to clay–polymer interactions.

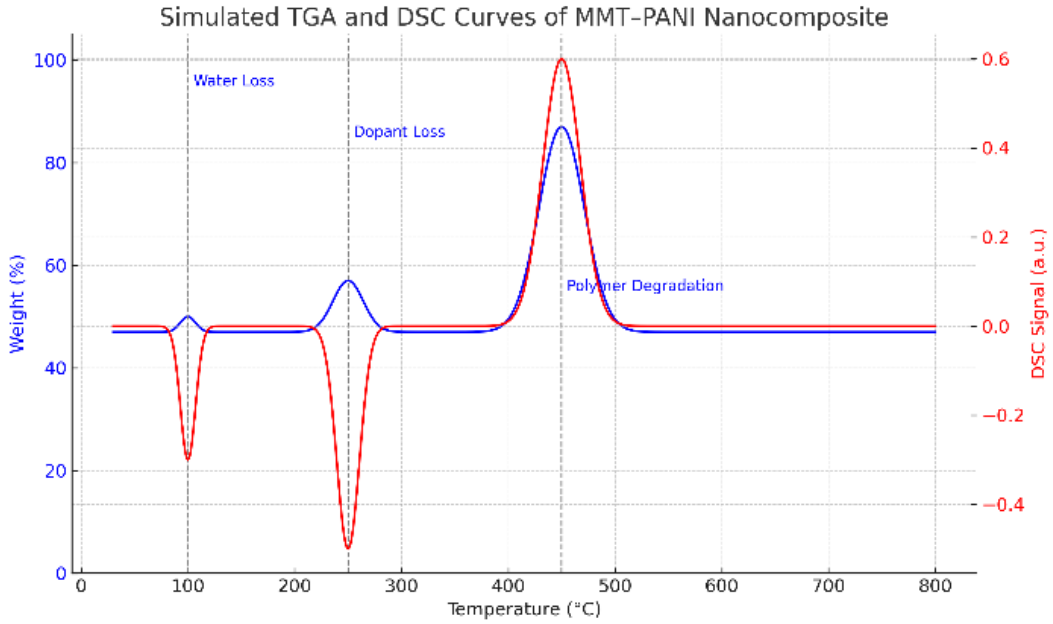

Figure 4. TGA/DSC of MMT–PANI showing moisture loss (~100 °C), dopant decomposition (~250 °C), and polymer degradation (~450 °C); no melting transition observed [63]

Table 3. Comparison between simulated TGA/DSC curves and features reported in the literature for MMT–PANI nanocomposites. References provide supporting experimental data

Thermal event	Simulated feature (from figure)	Reported feature (from literature)	Ref.
Water loss	Sharp TGA drop at ~100 °C with corresponding DSC endotherm	Initial weight loss below 120 °C is attributed to moisture evaporation	[64]
Dopant loss	Gradual TGA loss at ~250 °C with broad DSC endotherm	Weight loss between 200 and 300 °C due to dopant degradation	[12]
Polymer degradation	Major TGA loss at ~450 °C with sharp DSC exothermic peak	Main degradation between 400 and 500 °C from polyaniline backbone decomposition	[12]
Stability enhancement	—	PANI/MMT composites show delayed degradation to ~500–550 °C	[60,61]

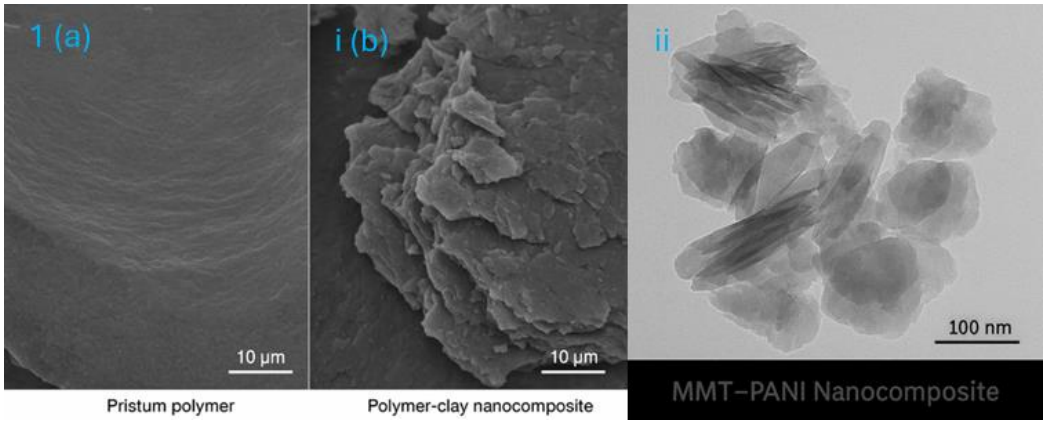

Figure 5. SEM and TEM images of MMT–PANI showing rough polymer-coated surfaces and exfoliated silicate layers [66]

Table 4. Comparative analysis of SEM and TEM images of MMT–PANI nanocomposites between simulated and published data. Structural features are aligned with morphology studies reported in literature

Image type	Simulated observation	Reported observation (Literature)	Ref.
SEM	Layered morphology with partially exfoliated clay structure and embedded granular PANI domains	SEM shows layered structure with rough surface and agglomerated polymer particles.	[8]
TEM	Intercalated/exfoliated lamellae with dark/light contrast indicating clay platelets and PANI matrix dispersion	TEM reveals intercalated silicate layers with polymer matrix in partially exfoliated morphology.	[53]

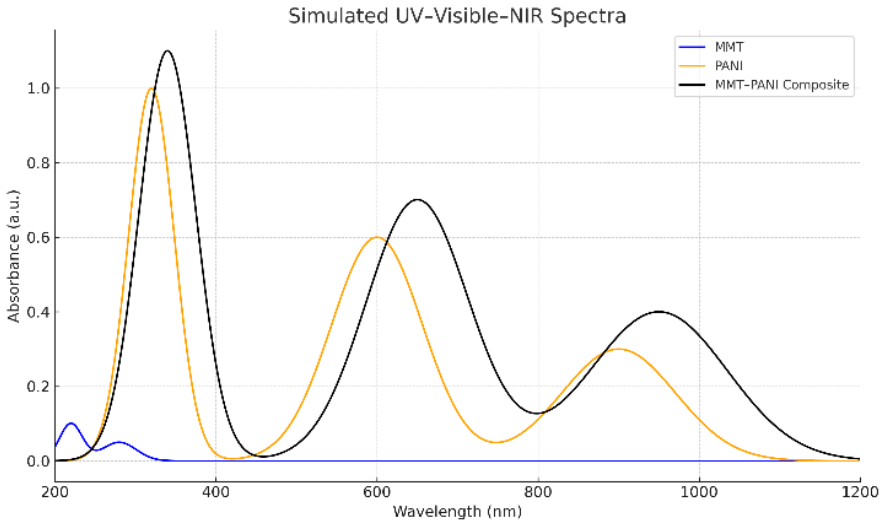

Figure 6. UV-Vis-NIR spectra of MMT, PANI, and MMT-PANI showing polymer-clay interactions and enhanced charge delocalisation [67]

The optical absorption behavior of pristine MMT, PANI, and their nanocomposite was studied using simulated UV–Vis–NIR spectra, as illustrated in **Figure 6**. Pristine MMT shows only weak absorption in the ultraviolet region (~220–280 nm), with little to no response in the visible or near-infrared regions, which aligns with its electronically inactive silicate structure [68]. In contrast, PANI displays a strong absorption peak at ~320 nm due to π–π* transitions in its benzenoid rings, a broad shoulder around ~600 nm linked to polaron–π* transitions, and a long absorption tail extending into the near-infrared (~900 nm), which signals the presence of delocalized charge carriers such as polarons and bi-polarons along its conjugated chain [69]. In the MMT–PANI nanocomposite, the absorption bands shift to longer wavelengths and broaden (observed at ~340 and ~650 nm), with increased absorption stretching into the NIR region up to 1100 nm. This redshift and spectral broadening suggest strong interfacial bonding between PANI chains and the clay surface, promoting better electronic delocalization and improved polaron mobility. These traits are particularly advantageous for applications in optoelectronic and photothermal devices [12]. **Table 5** provides a comparison of the simulated and literature-reported UV–Visible–NIR features for MMT, PANI, and their nanocomposite. The redshift and band broadening seen in the MMT–PANI nanocomposite highlight increased charge delocalization and strong clay–polymer interactions. Electrical conductivity is usually measured using either the two-point or four-point probe method, often under different temperature or pressure conditions. Adding clay to the polymer matrix can help fine-tune the conductivity by balancing interfacial resistance and percolation effects. For clay–polymer nanocomposites, electrical conductivity is often assessed using these probe techniques, where bulk PANI typically shows values between 10^{-4} and 10^{0} S/cm. Conductivity tends to follow Arrhenius behavior, increasing with temperature due to thermal activation.

When MMT clay is added at optimal levels-around 5 wt%—conductivity improves due to the formation of effective percolation pathways. However, adding too much clay can cause agglomeration, which lowers performance. Electrochemical impedance spectroscopy (EIS) is also used alongside DC measurements to identify parameters such as solution resistance (Rs), charge transfer resistance (Rct), double-layer capacitance (Cd), and Warburg diffusion (w). Reported Rct values generally range between 100 and 500 Ω, as shown in **Table 6**

[8,57,70,71]. Cyclic voltammetry (CV), electrochemical impedance spectroscopy (EIS), and galvanostatic charge-discharge (GCD) tests are employed to evaluate electrochemical behavior, particularly for applications in supercapacitors and sensors. CV curves help identify redox activity and reversibility, while EIS spectra break down charge transfer resistance (Rct), double-layer capacitance (Cdl), Warburg diffusion (W), and electrolyte resistance (Rs). GCD measurements are useful for estimating specific capacitance and coulombic efficiency. **Figure 7** presents the typical CV curves of polyaniline and its nanocomposite with montmorillonite.

Table 5. Comparison between simulated and literature-reported UV–Vis–NIR spectral features of MMT, PANI, and their nanocomposite. The red-shift and broadening in the composite spectrum indicate enhanced charge delocalisation and interaction between clay and polymer

Sample	Simulated spectral features	Reported spectral features	Ref.
Montmorillonite (MMT)	Weak absorption below 300 nm due to Si–O transitions	Low absorbance in UV-Vis region with weak bands < 300 nm	[69]
Polyaniline (PANI)	Peaks at ~330 nm (π–π* transition), ~620 nm (polaron–π*), and ~950 nm (bipolaron band)	~330–350 nm (π–π* transition), ~600–650 nm (polaron transitions), tailing into NIR region	[12]
MMT–PANI Composite	Enhanced and broadened bands at ~340 nm, ~660 nm, and ~980 nm indicating interfacial interactions and increased delocalisation	Broadened peaks with red-shift and increased NIR absorption due to improved conjugation and dispersion in nanocomposite	[12]
MMT: PANI (varied ratio)	Band shifts (~330 → 345 nm); NIR enhancement	Composition-dependent modulation; suppression of polaron band at high clay content	[60]
PANI/MMT/La^{3+}	π–π* shifted to ~360 nm; stronger polaron band at ~650–700 nm	Extended NIR absorption due to La-assisted charge transfer	[61]

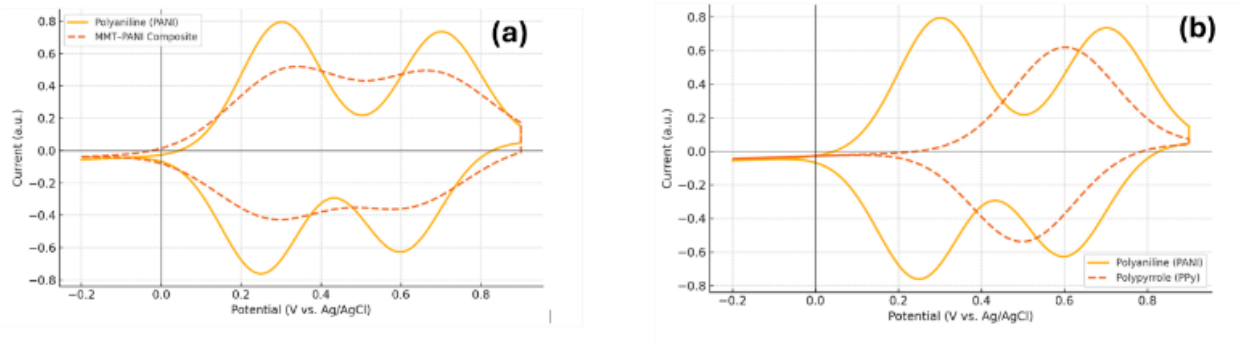

Figure 7. (a) Cyclic voltammograms (CV) of polyaniline (PANI) and MMT–PANI nanocomposite in 1 M H_2SO_4, scanned between −0.2 V and +0.9 V vs. Ag/AgCl and (b) cyclic voltammograms of polyaniline (PANI) and polypyrrole (PPy) recorded in 1 M H_2SO_4, scanned between −0.2 V and +0.9 V

Table 6. Quantitative summary of electrical conductivity measurement approaches, environmental effects, clay incorporation, and AC impedance parameters in clay–polymer nanocomposites, along with key references

Parameter	Description	Ref.
Measurement techniques	Four-point probe: 10^{-4}–10^{0} S cm^{-1} (bulk PANI); Two-point probe used for pellets and pressed films. Contact resistance minimised in four-point geometry.	[48]
Environmental conditions	Conductivity typically increases with temperature (Arrhenius behaviour); *e.g.,* 10^{-3} S cm^{-1} at 30°C → 10^{-2} S cm^{-1} at 80 °C for clay–PANI composites.	[70]
Effect of Clay incorporation	MMT loading ~5 wt% enhances conductivity from 10^{-4} to ~10^{-2} S cm^{-1} by improving percolation; excess loading decreases due to agglomeration.	[64]
AC Impedance spectroscopy (EIS)	Nyquist plots show semicircles and Warburg lines; Rs ~20 Ω, Rct ~100–500 Ω; Bode plots reflect frequency-dependent conductivity and capacitance.	[60,61]

Pristine PANI shows two clear redox peaks that correspond to its stepwise oxidation and reduction. However, in the MMT–PANI composite, these redox signals become broader and less pronounced, indicating that the presence of clay affects charge transport and overall electrochemical performance [8,12,57]. The cyclic voltammograms (CVs) of polyaniline (PANI) and PPy in 1 M H_2SO_4 exhibit distinct electrochemical behaviours due to fundamental differences in their redox mechanisms and molecular structures. PANI displays two well-defined pairs of redox peaks, corresponding to its stepwise oxidation from leucoemeraldine to emeraldine and then to pernigraniline, and the reverse transitions upon reduction (for example, **Figure 7**- The PANI spectrum shows two oxidation peaks (~0.3 V and ~0.7 V) corresponding to leucoemeraldine to emeraldine and emeraldine to pernigraniline transitions, respectively, along with two reduction peaks in the reverse scan). These discrete transitions reflect the polymer's partially rigid conjugated backbone, which supports stable intermediate oxidation states. In contrast, PPy exhibits a single broad and more reversible redox couple, indicative of a continuous doping/dedoping process involving counter-ion exchange, rather than distinct oxidation states (for example, **Figure 7**(a)- The MMT–PANI composite exhibits broadened and less intense redox peaks, attributed to interfacial resistance and reduced electroactive surface area due to clay incorporation and **Figure 7**(b)- PPy shows a single broad redox couple (~0.6 V oxidation, ~0.5 V reduction), indicative of a continuous and reversible doping/dedoping process. The broader peaks and enhanced capacitive background in PPy reflect its pseudocapacitive behavior and greater ionic mobility compared to PANI). This broadness is further accentuated by the greater swelling and ion diffusion effects in PPy, which lead to higher capacitive currents and pseudocapacitive behavior. Consequently, PANI demonstrates more Faradaic character with quasi-reversible redox peaks, while PPy exhibits smoother, diffusion-influenced voltammograms with enhanced capacitive contributions. These differences underline the distinct electrochemical signatures and charge storage mechanisms of the two polymers. Atomic force microscopy (AFM) and X-ray photoelectron spectroscopy (XPS) are also used to examine surface roughness, local conductivity, and chemical states, providing valuable complementary insights into nanoscale interactions. **Figure 8** shows simulated AFM

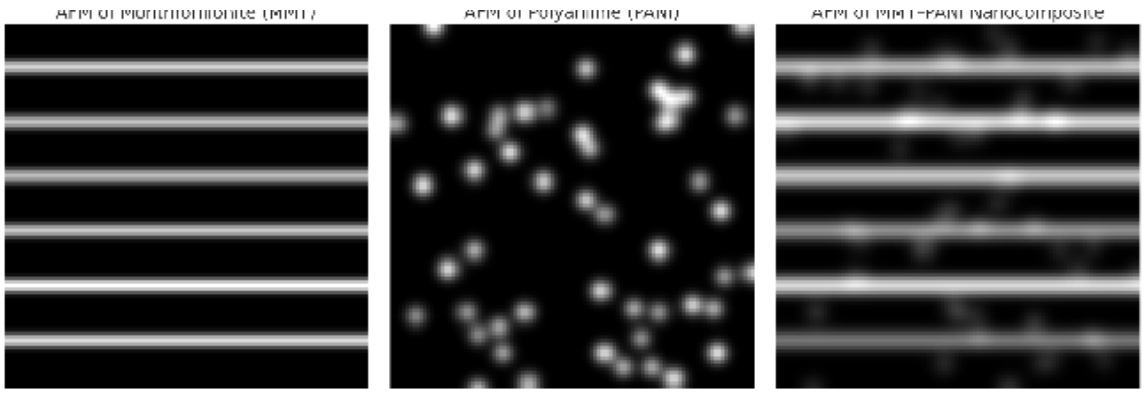

Figure 8. Simulated atomic force microscopy (AFM) images of (a) pristine montmorillonite (MMT), (b) polyaniline (PANI), and (c) MMT–PANI nanocomposite. The MMT image shows a characteristic layered morphology with stacked platelets and relatively flat terraces. PANI appears as a granular film with nodular polymer domains due to irregular electro-polymerisation. The MMT–PANI composite reveals a hybrid topography featuring clay lamellae embedded in the polymer matrix, indicating partial intercalation and surface coverage by PANI

images that highlight the different surface morphologies of MMT, PANI, and their nanocomposite.

Pristine MMT reveals layered structures characteristic of stacked silicate platelets, while the PANI film displays globular domains that result from its granular polymer growth. The nanocomposite image shows a combination of these features, indicating interactions between clay and polymer and partial surface coverage. This mixed morphology aligns well with AFM findings reported in previous studies on similar systems [8,72,73]. Electrochemical impedance spectroscopy (EIS) is a valuable method for studying interfacial charge transport, ion diffusion, and capacitive behavior in clay–conducting polymer (CP) nanocomposites. Typically recorded over a frequency range from 1 MHz to 1 mHz, impedance spectra often feature a high-frequency intercept (solution resistance, R_s), a semicircular region (reflecting the parallel combination of charge transfer resistance, R_{ct}, and double-layer capacitance, C_{dl}), and a low-frequency tail representing Warburg impedance (W), which signals ionic diffusion through the porous structure [12,74].
When exfoliated or intercalated clays such as Na^+-montmorillonite or Laponite are added to PANI or PPy, they reshape ion transport paths, expand the interfacial area, and reduce R_{ct} by improving dispersion and ion accessibility [32]. This effect also appears in Bode plots, where higher phase angles and broader frequency-dependent capacitance profiles point to better capacitive performance. Using equivalent circuit models like modified Randles or transmission line models, R_s, R_{ct}, and Cdl values can be extracted. Clay platelets also increase pseudocapacitive effects by buffering ions and promoting electron hopping at the interfaces [12]. These traits are especially beneficial in supercapacitors, biosensors, and flexible energy storage devices, where performance depends on a good mix of conductivity, capacitance, and durability. **Figure 9** shows a simulated Nyquist plot capturing the typical features of electrochemical impedance: starting with Rs on the real axis, followed by a semicircle representing R_{ct}–C_{dl}, then a 45° line due to Warburg diffusion, and finally a vertical capacitive tail. This idealized curve closely matches real EIS patterns reported for polyaniline and its nanocomposites containing clay or carbon fillers [12,13,70]. The EIS data, visualized through Nyquist and Bode plots, outlines the step-by-step behavior of charge transport and interfacial processes in a standard electrode–electrolyte system. The Nyquist plot starts with a horizontal intercept (Rs), then a

semicircle tied to R_{ct} and C_{dl} (Faradaic kinetics), followed by a 45° line due to Warburg diffusion, and ends with a near-vertical segment showing ideal capacitive behavior at low frequencies. The Bode magnitude plot features three clear regions: a flat high-frequency zone (Rs), a rising mid-frequency region (R_{ct}–C_{dl}), and a steep slope at low frequencies from diffusion and capacitance. The Bode phase plot reflects this too—starting at 0° (resistive), dipping to –45° (semi-Faradaic), and nearing –90° at low frequencies (capacitive). Altogether, these plots provide a complete picture of how complex systems such as PANI and its clay nanocomposites respond across frequencies (**Figure 10**). The way R_{ct} and C_{dl} change with DC potential bias offers key insights into the electrochemical switching behavior of the MMT–PPY nanocomposite. When the bias is low—around 0 mV and ±200 mV—Rct is high, indicating poor electronic conductivity due to the PPy matrix being in an undoped or partially doped state. In this range, the polymer is mostly in its insulating or semiconducting form, leading to limited electron transfer at the electrode–electrolyte interface. As the bias shifts further positive or negative (beyond ±600 mV), R_{ct} decreases significantly, signaling the start of Faradaic processes and PPy's electrochemical doping/dedoping. In these regions, the polymer's backbone undergoes oxidation or reduction, boosting charge mobility and reducing interface resistance. This shift from insulating to conducting behavior with applied bias is a hallmark of conducting polymers. Meanwhile, C_{dl} changes more gradually. It tends to be slightly higher at intermediate biases (around ±400 mV to ±600 mV), likely due to increased charge carrier density and better ion access.

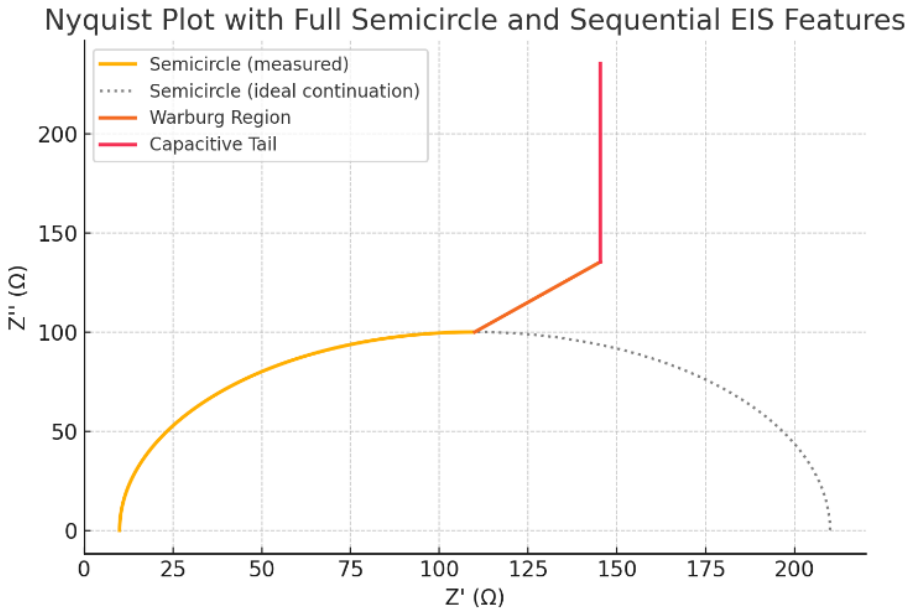

Figure 9. Idealised Nyquist plot showing the sequential impedance response of a typical electrochemical system comprising (i) an initial intercept at Z′ = R_s (solution resistance), followed by (ii) a semicircle representing the charge transfer resistance (R_{ct}) and double-layer capacitance (C_d), (iii) a 45° Warburg line indicating ion diffusion, and (iv) a vertical tail at low frequencies attributed to ideal capacitive behaviour. The dotted lower half of the semicircle illustrates the full arc of the R_{ct}//C_d circuit for visual completeness

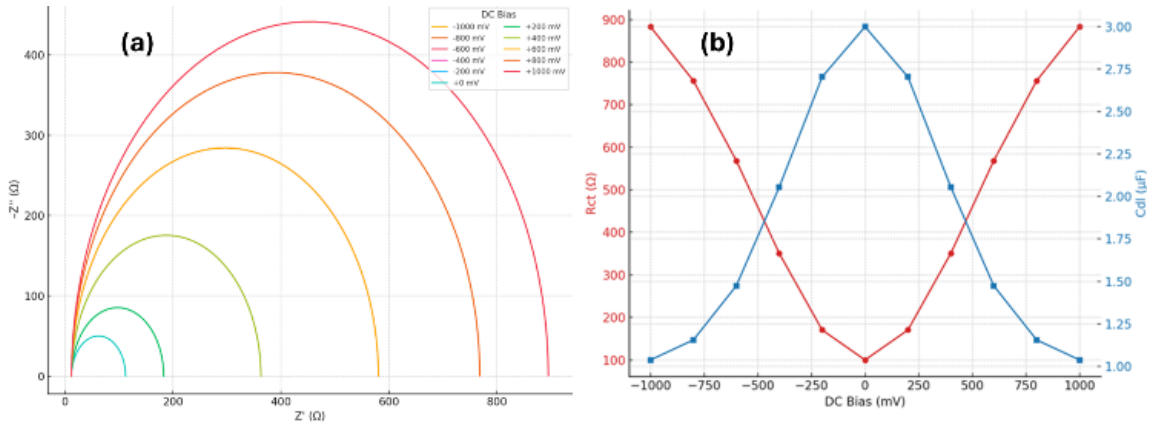

Figure 10. (a) Nyquist plots of MMT–PPy under ±1,000 mV bias showing R_{ct}//C_{dl} minima at extremes and maximum near 0 mV; (b) Rct (red) and Cdl (blue) vs. bias, with R_{ct} minima at high |V| and C_{dl} peaking at intermediate potentials [63]

At extreme potentials (±1,000 mV), the drop in Cdl may result from a tighter electrical double layer or steric effects caused by excessive ion buildup or structural shifts in the polymer. Clay–conducting polymer (CP) nanocomposites show improved mechanical performance thanks to the nanoconfinement effect and reinforcement from the high-aspect-ratio silicate layers. Mechanical characteristics like tensile strength, Young's modulus, and elongation at break are usually measured through standard tensile tests. For example, adding 3–5 wt% montmorillonite to PANI can boost tensile strength by more than 50% and increase the modulus by over 100% compared to the neat polymer [58]. Dynamic mechanical analysis (DMA) further reveals higher storage moduli and elevated glass transition temperatures (T_g), which suggest restricted polymer chain mobility due to strong adhesion between the polymer and clay surfaces [62]. The level of mechanical improvement strongly depends on factors such as the exfoliation of clay, compatibility between clay and polymer, and the method used for processing. For flexible applications—such as wearable electronics or soft actuators—clay–polymer nanocomposites offer excellent durability, withstanding repeated bending and stretching without failure. This is mainly due to the crack-arresting role of the silicate layers and better stress transfer within the nanocomposite [59].

The mechanical traits of MMT, PPy, and their composite (MMT–PPy) reveal distinct but complementary behaviors. MMT is a stiff silicate clay, with a high Young's modulus (~5.0 GPa), but it lacks flexibility, shown by its low elongation at break (~2%) and moderate tensile strength (~20 MPa). PPy, on the other hand, is quite ductile, with a high elongation at break (~30%) and strong tensile strength (~45 MPa); although its stiffness is low (~0.2 GPa). When these are combined into an MMT–PPy nanocomposite, the resulting material shows a balance of properties: it has a modulus of ~1.5 GPa (thanks to clay reinforcement), and it retains better flexibility and strength (~10% elongation and ~35 MPa strength) than pure MMT. This performance improvement comes from the synergy between PPy's flexibility and MMT's reinforcing ability, helping the composite strike a good balance between stiffness, strength, and ductility (**Figure 11**).

5. Applications of Montmorillonite - Electrically Conducting Polymer (MMT-ECP) Nanocomposites

5.1. Applications for supercapacitors

Montmorillonite–electrically conducting polymer (MMT–ECP) nanocomposites emerged as promising electrode materials for supercapacitors because of their large surface

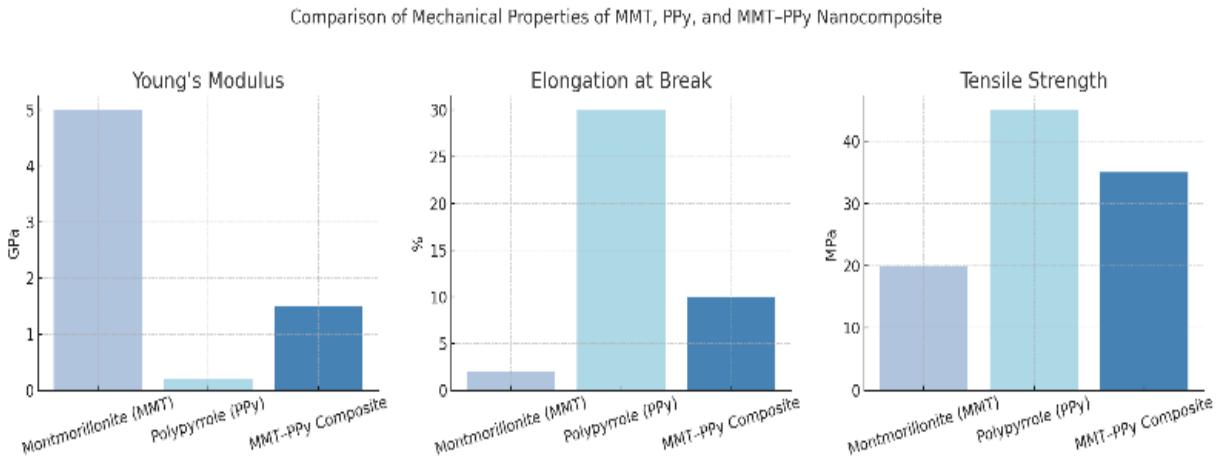

Figure 11. Mechanical properties of MMT, PPy, and MMT–PPy nanocomposite showing enhanced modulus, strength, and ductility [68]

area, redox-active properties, and improved mechanical strength. Conducting polymers such as PANI, PPy, and PEDOT provide pseudocapacitance through Faradaic redox reactions, while the intercalated or exfoliated MMT layers offer structural support and allow ions to move through easily. This combination results in better specific capacitance, stability over cycles, and enhanced mechanical integrity compared to pristine polymers. The mechanism of charge storage in these composites is twofold: (i) redox reactions occurring within the conjugated polymer backbone, and (ii) ion buffering and adsorption provided by the intercalated or exfoliated clay layers.

The clay platelets act as spacers that prevent polymer chain aggregation, increasing the accessible electroactive surface area and enabling more effective electrolyte penetration. Additionally, MMT provides mechanical stability that suppresses volumetric changes of the polymer during doping/dedoping, thereby extending cycling life. Several studies have reported superior electrochemical performance for MMT–ECP nanocomposites compared to their pristine polymer counterparts. For example, Rajapakse and Murakami [9] found that PPy–MMT nanocomposites used as cathodes for oxygen reduction had improved charge storage and electrochemical stability. Yan *et al.* [75] demonstrated that clay-based nanocomposites reached specific capacitances over 300 $F \cdot g^{-1}$ and retained more than 90% of their capacitance after 5,000 cycles, showing strong long-term performance in water-based electrolytes. The high cation-exchange capacity of MMT plays a pivotal role here, as it promotes rapid ion diffusion during charge–discharge, thus maintaining stable capacitance at high current densities. helps with ion movement during charging and discharging, while its layered structure prevents the polymer from swelling or cracking. Although the electrical conductivity of these nanocomposites is lower than that of carbon-based nanomaterials, MMT–ECP nanocomposites offer distinct advantages including tunable redox activity, low cost, environmental compatibility, and mechanical robustness. When combined with conductive additives such as carbon nanotubes or graphene, the conductivity barrier can be overcome, further enhancing rate performance. Because of these attributes, MMT–ECP nanocomposites are increasingly considered for the development of flexible, solid-state, and wearable supercapacitors, where mechanical stability, affordability, and eco-friendliness are as critical as energy density.

Table 7. EMI shielding performance of selected MMT–ECP nanocomposites

Composite system	MMT content (wt%)	Shielding effectiveness (dB)	Frequency range (GHz)	Ref.
Polyaniline/MMT	10	30–35	8–12 (X-band)	[64]
Polypyrrole/MMT	5	28–32	8–12	[76]
PEDOT/MMT	7	25–30	8–10	[77]

5.2. EMI shielding performance of MMT-ECP nanocomposites

Electromagnetic interference (EMI) is a growing concern in modern electronics, aerospace, and wearable devices, where compact and high-frequency circuits are increasingly vulnerable to unwanted electromagnetic radiation. MMT–ECP nanocomposites are gaining attention as effective materials for electromagnetic interference (EMI) shielding, thanks to their unique mix of dielectric, conductive, and reflective properties. The mechanism of shielding involves absorption, reflection, and multiple scattering of electromagnetic waves. Montmorillonite layers increase the effective path length of incident radiation, forcing multiple reflections and enhancing absorption. Meanwhile, the conducting polymer matrix—such as polyaniline or polypyrrole—helps dissipate the induced currents as heat through electronic conduction and interfacial polarization. This dual contribution provides broad-spectrum EMI attenuation. Performance studies highlight the potential of these materials. Harshitha and Ramakrishna [18] demonstrated that adding just 5–10 wt% MMT to these polymers significantly boosted shielding effectiveness (SE), reaching values over 30 dB. This is enough to block more than 99.9% of incoming radiation in the X-band (8–12 GHz). The improvement comes from a combination of interfacial polarization, multiple reflections inside the clay layers, and better impedance matching due to the hybrid structure. These results are remarkable considering the composites are lighter, corrosion-resistant, and more flexible compared to traditional metal-based shields (**Table 7**). Although their conductivity is lower than carbon nanofiller systems, MMT–ECP nanocomposites offer superior processability and reduced costs. Moreover, their performance can be tuned by aligning clay platelets or functionalizing their surfaces to improve impedance matching at specific frequencies. This makes MMT–ECP composites ideal for EMI shielding in applications such as consumer electronics, aerospace, flexible circuits, and wearable devices.

5.3. Applications in solid state batteries

Solid-state batteries (SSBs) require materials that can efficiently transport both ions and electrons while maintaining mechanical and thermal stability. Montmorillonite–conducting polymer (MMT–ECP) nanocomposites are drawing increasing interest for use as solid polymer electrolytes (SPEs) [78] and electrode materials in next-generation SSBs, thanks to their combined benefits of ionic conductivity, structural strength, and electrochemical stability. The mechanism is twofold: (i) montmorillonite disrupts the crystallinity of host polymers such as polyethylene oxide (PEO), increasing segmental chain mobility and thus enhancing ionic conductivity, and (ii) ECPs create percolated electronic pathways that accelerate charge transfer at the electrode–electrolyte interface. Additionally, the clay platelets act as mechanical barriers against lithium dendrite penetration, improving battery safety. Performance reports are promising. Thomas *et al.* [10] observed that adding 5–10 wt% MMT to PEO-based electrolytes increased lithium-ion conductivity from ~10^{-7} to 10^{-5} S/cm at room temperature. Blends of MMT–PANI have achieved conductivities above 10^{-3} S/cm at 60–80 °C, approaching the threshold required for practical SSB operation [11]. The

layered MMT not only aids in ion separation and transport, but also strengthens the material mechanically, helping to stop lithium dendrites from forming. Moreover, the electroactive nature of ECPs allows these nanocomposites to serve as hybrid cathodes, adding pseudocapacitance and speeding up charge transfer which stands out for its low cost, flexibility, and scalability. Their hybrid electronic–ionic transport properties make them strong candidates for use in wearable electronics, electric vehicles, and grid-scale storage devices. Future research should emphasize optimizing clay dispersion and polymer–clay interfacial bonding to achieve higher room-temperature conductivity and long-term cycling stability.

5.4. Applications in chemical sensing

Chemical sensing requires materials that are sensitive, selective, and stable under varying environmental conditions. Montmorillonite–electrically conducting polymer (MMT–ECP) nanocomposites hold strong potential for chemical sensing because they combine a large surface area, redox activity, and good interfacial conductivity. The sensing mechanism typically involves conductivity or potential changes in the polymer upon interaction with target analytes. Montmorillonite enhances this by providing high surface area, selective adsorption sites, and a platform for immobilizing catalytic species or biomolecules. This results in enhanced sensitivity, faster response times, and broader detection ranges. Meanwhile, the MMT adds structural support and improves sensitivity by selectively adsorbing certain molecules. Reported applications include detection of gases (NH_3 and NO_2), heavy metals, and organic contaminants. Krishantha and Rajapakse [11] developed Cu^+-conducting polypyrrole–MMT nanocomposites that can detect redox-active species with impressive selectivity and consistency. The clay layers help evenly distribute the polymer and make it easier to attach catalytic or sensing agents. These nanocomposites also respond quickly and can detect low concentrations of harmful gases (such as NH_3 and NO_2), heavy metals, and organic contaminants. Their compatibility with screen printing and drop-casting makes them ideal for low-cost or flexible sensor designs. In biosensing, enzymes or antibodies can be added to the clay–polymer structure to further improve specificity while maintaining good electron transfer. Due to their adjustable redox potential and balanced hydrophilic–hydrophobic nature, MMT–ECP films are excellent for developing multi-analyte sensors and electrochemical devices used in environmental monitoring, food safety, and medical diagnostics. Although their detection limits and selectivity are not always as high as advanced nanocarbon-based sensors, MMT–ECP nanocomposites offer significant advantages in cost, scalability, and multifunctionality. With further optimization, they can be integrated into flexible, printed sensor platforms for environmental monitoring, food safety, and medical diagnostics.

5.5. Applications in flexible and wearable electronics

The rapid growth of wearable and flexible devices demands materials that combine electronic conductivity with mechanical robustness and environmental durability. Montmorillonite–electrically conducting polymer (MMT–ECP) nanocomposites are well-suited for this role, as they retain electrical conductivity along with mechanical strength and environmental durability. Conducting polymers such as PPy, PANI, and PEDOT offer tunable conductivity and electrochemical activity, while MMT adds strength, flexibility, and makes the materials easier to process into thin films or coatings. The exfoliated MMT layers also reduce the movement of the polymer chains, which strengthens the material and prevents it from breaking down when bent or stretched repeatedly. The mechanism is based on exfoliated MMT layers restricting excessive polymer chain motion, thereby reducing cracking and enhancing durability under bending or stretching. Conducting polymers supply electroactivity and processability in thin

films, while the clay improves adhesion to flexible substrates. Singh and Verma showed that flexible MMT–PANI composite films could maintain conductivity between 10^{-1} and 10^{-2} $S \cdot cm^{-1}$ even after more than 1,000 bending cycles—ideal for wearable electronics and bendable circuits [79]. These films adhere well to fabrics and perform reliably under normal environmental conditions. MMT's heat resistance also helps prevent the polymer from degrading during use or heat treatments. These composites have been used as flexible sensors, touchscreens, energy-harvesting clothing, and antistatic layers in smart wearables. Because they can be printed or sprayed on surfaces, MMT–ECP composites are especially attractive for creating affordable, large-area wearable electronics.

The main limitation is their lower conductivity compared to metallic inks, but this can be improved by hybridizing with carbon nanotubes, graphene, or metallic nanoparticles. Future directions include integration into energy-harvesting textiles, flexible sensors, and self-powered devices, emphasizing their role in next-generation smart wearables.

5.6. Applications in water purification

Clean water access is a global challenge, and MMT–ECP nanocomposites provide a sustainable route for pollutant removal due to their synergistic adsorption and electrochemical functions. Montmorillonite offers high surface area and ion-exchange ability with the redox activity and conductivity of conducting polymers. These materials can act both as effective adsorbents and as electrochemical agents for removing heavy metals, dyes, fluoride, arsenic, and other tough pollutants from water. The mechanism involves electrostatic adsorption of ions and organic molecules onto the clay surface, combined with reduction/oxidation of pollutants by the polymer backbone. This dual functionality improves removal efficiency and allows for reusability through electrochemical regeneration. Rajapakse *et al.* have shown that polyaniline–MMT and polypyrrole–clay composites can remove Cr (VI), Pb (II), and fluoride much more efficiently and quickly than using just the clay or the polymer alone [8,13,80]. The redox-active polymer helps reduce metal ions and absorb charged pollutants, while the clay layers support fast ion transport and structural strength. Jayawardana and Rajapaks [14] reported that MMT–polyaniline materials removed over 90% of textile dyes and could be reused several times. These nanocomposites can be made into pellets, membranes, or coated electrodes, allowing for easy integration into filtration systems, capacitive deionization units, or electrochemical treatment devices. Compared to activated carbon or resins, MMT–ECP nanocomposites offer the advantages of low cost, higher stability, and the possibility of selective electrochemical regeneration. Their eco-friendliness, and ability to be regenerated make them a strong choice for decentralized water treatment, especially in areas with limited resources.

5.7. Applications in barrier and packaging materials

The packaging industry requires materials with excellent barrier properties against gases, vapors, and light, alongside additional functionalities such as antistatic behavior and microbial resistance. Montmorillonite–electrically conducting polymer (MMT–ECP) nanocomposites are drawing a lot of attention in the packaging industry as next-generation barrier materials, thanks to their ability to block gases, moisture, and volatile substances. The thin plate-like structure of montmorillonite creates a complex path that slows down the movement of molecules, while the conducting polymers—such as PANI or PPy—add useful features such as antistatic, antimicrobial, and sensing abilities. This combination leads to films with much lower oxygen and water vapor transmission rates (OTR and WVTR), making them ideal for packaging food, medicine, and electronics. For example, Rhim and demonstrated that poly(vinyl alcohol) (PVA)/MMT films reduced water permeability by 40–60%, and when mixed with ECPs, the

films also gained electrical conductivity (~10^{-3} S·cm^{-1}) and UV-blocking properties. These materials are not only eco-friendly and biodegradable, but also align with sustainable packaging goals. The electroactive nature of ECPs even allows for intelligent packaging that can react to changes in the environment—such as shifts in temperature, pH, or gas levels—to help monitor shelf life or signal product quality. Manufacturing techniques like solution casting, extrusion, and multilayer lamination make it feasible to produce these films on a large scale, reinforcing their commercial promise for smart packaging.

5.8. Biomedical applications

Biomedical engineering increasingly relies on materials that are biocompatible, electroactive, and tunable. MMT–electrically conducting polymer (ECP) nanocomposites are gaining momentum in biomedical fields such as drug delivery, tissue engineering, biosensing, wound healing, and antimicrobial coatings. The mechanism of their biomedical function depends on both components: montmorillonite clay offers biocompatibility, high surface area, and ion-exchange properties, helping it interacts well with biological systems and drugs. Meanwhile, conducting polymers such as polypyrrole and polyaniline provide electroactivity, redox responsiveness, and flexibility—features that are crucial in dynamic biological environments. Examples include PANI–MMT carriers for anticancer drugs, which release therapeutic agents in response to pH or electrical stimuli, and chitosan–MMT–ECP scaffolds that enhance osteoblast adhesion and growth for bone and cartilage regeneration. Darder *et al.* [22] showed that these bio-nanocomposites could carry anticancer drugs and release them in a controlled manner in response to changes in pH or electrical signals. Zhuang and Lin [25] developed chitosan–clay scaffolds enhanced with ECPs for bone and cartilage regeneration, which supported better cell growth and development. These composites can even mimic the electrical characteristics of tissues like nerves or the heart, making them ideal for electrically responsive implants and tissue scaffolds. Additionally, their natural antibacterial effects—due to both the oxidative nature of ECPs and the ion-exchange ability of MMT—make them excellent for wound dressings and implant coatings. They can be easily shaped into films, hydrogels, or 3D porous structures, adding to their flexibility for medical use. With further fine-tuning of functionality and safety, MMT–ECP nanocomposites hold strong promise for the next wave of biomedical technologies. Future research should focus on biodegradable ECPs combined with clays, to create transient implants that degrade safely in the body while delivering therapeutic benefits.

6. Conclusion and Outlook

Clay–conducting polymer nanocomposites (CPNs), especially those based on montmorillonite (MMT) and conductive polymers like polyaniline, polypyrrole, and PEDOT, are emerging as highly versatile materials. Their mix of strong mechanical properties, electrical conductivity, and customizable surface features has placed them at the center of innovation in green and sustainable technologies. This review has tracked their evolution—from simple electroactive films to a wide range of uses in energy storage, environmental clean-up, healthcare, and smart packaging. A key takeaway from current research is the importance of their nanostructure—particularly how well the clay is dispersed or intercalated—which heavily influences performance. The methods used to make these materials, such as *in situ* polymerization, solution blending, or electrochemical deposition, play a significant role in shaping their structure and functionality. Thanks to advanced testing methods, a clearer picture of how structure links can be obtained to performance, paving the way for smarter material design. Still, some areas need more attention. Biomedical and smart packaging applications are full of untapped potential—especially if bio-based polymers and eco-friendly production methods can be utilized. Making these materials more scalable, reliable,

and stable under real-world conditions will be crucial for wider adoption. Looking ahead, combining green chemistry, 3D printing, and nature-inspired designs could open new frontiers for CPNs. Future studies should also examine closely at their full life cycle, recyclability, and how well they meet environmental and safety standards—key aspects for making them part of a circular economy. By linking strong science with practical innovation, MMT–ECP nanocomposites are well-positioned to shape a more sustainable future across multiple sectors.

Acknowledgements

This research work was financially supported by INTI International University, Malaysia (HO SM).

Conflicts of Interest

No conflicts to declare were reported by the authors in this study.

Data Availability

The data supporting of the findings of this study are available within the article.

Orcid

R.M.G. Rajapakse
https://orcid.org/0000-0003-3943-5362

Theekshana Malalagama
https://orcid.org/0009-0003-2519-3822

V.M.Y.S.U. Bandara
https://orcid.org/0009-0009-4693-7708

Ho Soonmin
https://orcid.org/0000-0002-3697-5091

References

[1]. Srinivas, S., Ananthapadmanabha, G., Suresha, B., Nagarajan, R., Mohammad, F., Krishnan, K., Devi, M.I., Ahmad, S., Experimental studies on the physical and mechanical properties of modified silica/graphene reinforced polyamide6/copolyester elastomer blend nanocomposites. *Polymer Engineering & Science*, **2025**, 65(2), 605-619.
[2]. Uddin, M.N., Hossain, M.T., Mahmud, N., Alam, S., Jobaer, M., Mahedi, S.I., Ali, A., Research and applications of nanoclays: A review. *SPE Polymers*, **2024**, 5(4), 507-535.
[3]. Guo, F., Aryana, S., Han, Y., Jiao, Y., A review of the synthesis and applications of polymer–nanoclay composites. *Applied Sciences*, **2018**, 8(9), 1696.
[4]. Nezakati, T., Seifalian, A., Tan, A., Seifalian, A.M., Conductive polymers: Opportunities and challenges in biomedical applications. *Chemical reviews*, **2018**, 118(14), 6766-6843.
[5]. Sun, Z., Ou, Q., Dong, C., Zhou, J., Hu, H., Li, C., Huang, Z., Conducting polymer hydrogels based on supramolecular strategies for wearable sensors. *Exploration*, **2024**, 4(5), 20220167.
[6]. Vaia, R.A., Giannelis, E.P., Polymer nanocomposites: Status and opportunities. *MRS Bulletin*, **2001**, 26(5), 394-401.
[7]. Wu, L., He, X., Zhao, Y., Huang, K., Tong, Z., Liao, B., Pang, H., Montmorillonite-based materials for electrochemical energy storage. *Green Chemistry*, **2024**, 26(2), 678-704.
[8]. Rajapakse, R., Murakami, K., Bandara, H., Rajapakse, R., Velauthamurti, K., Wijeratne, S., Preparation and characterization of electronically conducting polypyrrole-montmorillonite nanocomposite and its potential application as a cathode material for oxygen reduction. *Electrochimica Acta*, **2010**, 55(7), 2490-2497.
[9]. Wijeratne, W., Rajapakse, R., Wijeratne, S., Velauthamurty, K., Thermal properties of montmorillonite–polyaniline nanocomposites. *Journal of Composite Materials*, **2012**, 46(11), 1335-1343.
[10]. Kazim, S., Ahmad, S., Pfleger, J., Plestil, J., Joshi, Y.M., Polyaniline–sodium montmorillonite clay nanocomposites: Effect of clay concentration on thermal, structural, and electrical properties. *Journal of Materials Science*, **2012**, 47(1), 420-428.
[11]. Krishantha, D., Rajapakse, R., Tennakoon, D., Bandara, W., Thilakarathna, P.L., Cuprous ion conducting montmorillonite-polypyrrole nanocomposites. *Solid state Ionics: Advanced Materials for Emerging Technologies*, **2006**, 170-178.
[12]. Rajapakse, R., Rajapakse, R., Bandara, H., Karunarathne, B., Electrically conducting polypyrrole–fuller's earth nanocomposites: Their preparation and characterisation. *Electrochimica acta*, **2008**, 53(6), 2946-2952.
[13]. Soundararajah, Q., Karunaratne, B., Rajapakse, R., Montmorillonite polyaniline nanocomposites: Preparation, characterization and investigation of

mechanical properties. *Materials Chemistry and Physics*, **2009**, 113(2-3), 850-855.
[14]. Senarathna, K., Randiligama, H.M., Rajapakse, R., Preparation, characterization and oxygen reduction catalytic activities of nanocomposites of co (ii)/montmorillonite containing polypyrrole, polyaniline or poly (ethylenedioxythiophene). *RSC Advances*, **2016**, 6(114), 112853-112863.
[15]. Senarathna, K.C., Mantilaka, M., Peiris, T.N., Pitawala, H., Karunaratne, D., Rajapakse, R., Convenient routes to synthesize uncommon vaterite nanoparticles and the nanocomposites of alkyd resin/polyaniline/vaterite: The latter possessing superior anticorrosive performance on mild steel surfaces. *Electrochimica Acta*, **2014**, 117, 460-469.
[16]. Ghafarloo, S., Kokabi, M., Mechanical properties of epoxy clay nanocomposites. *Advanced Materials Research*, **2010**, 123, 145-148.
[17]. Sumdani, M.G., Islam, M.R., Yahaya, A.N.A., Safie, S.I., Recent advancements in synthesis, properties, and applications of conductive polymers for electrochemical energy storage devices: A review. *Polymer Engineering & Science*, **2022**, 62(2), 269-303.
[18]. Zhang, L., Zhang, W.B., Chai, S.S., Han, X.W., Zhang, Q., Bao, X., Guo, Y.W., Zhang, X.L., Zhou, X., Guo, S.B., Clay mineral materials for electrochemical capacitance application. *Journal of The Electrochemical Society*, **2021**, 168(7), 070558.
[19]. Yan, J., Wang, Q., Wei, T., Fan, Z., Recent advances in design and fabrication of electrochemical supercapacitors with high energy densities. *Advanced Energy Materials*, **2014**, 4(4), 1300816.
[20]. Shunmugasamy, V.C., Xiang, C., Gupta, N., Clay/polymer nanocomposites: Processing, properties, and applications. *Hybrid and Hierarchical Composite Materials*, **2015**, 161-200.
[21]. Avella, M., De Vlieger, J.J., Errico, M.E., Fischer, S., Vacca, P., Volpe, M.G., Biodegradable starch/clay nanocomposite films for food packaging applications. *Food Chemistry*, **2005**, 93(3), 467-474.
[22]. Darder, M., Aranda, P., Ruiz-Hitzky, E., Bionanocomposites: A new concept of ecological, bioinspired, and functional hybrid materials. *Advanced materials*, **2007**, 19(10), 1309-1319.
[23]. Yao, J., Mao, L., Wang, C., Liu, X., Liu, Y., Development of chitosan/poly (vinyl alcohol) active films reinforced with curcumin functionalized layered clay towards food packaging. *Progress in Organic Coatings*, **2023**, 182, 107674.
[24]. Wijesinghe, W., Mantilaka, M., Peiris, T.N., Rajapakse, R., Wijayantha, K.U., Pitawala, H., Premachandra, T., Herath, H., Rajapakse, R., Preparation and characterization of mesoporous hydroxyapatite with non-cytotoxicity and heavy metal adsorption capacity. *New Journal of Chemistry*, **2018**, 42(12), 10271-10278.
[25]. Ateh, D., Navsaria, H., Vadgama, P., Polypyrrole-based conducting polymers and interactions with biological tissues. *Journal of The Royal Society Interface*, **2006**, 3(11), 741-752.
[26]. Kenry, Liu, B., Recent advances in biodegradable conducting polymers and their biomedical applications. *Biomacromolecules*, **2018**, 19(6), 1783-1803.
[27]. Balint, R., Cassidy, N.J., Cartmell, S.H., Conductive polymers: Towards a smart biomaterial for tissue engineering. *Acta Biomaterialia*, **2014**, 10(6), 2341-2353.
[28]. Zhang, Y.L., Li, J.C., Zhou, H., Liu, Y.Q., Han, D.D., Sun, H.B., Electro-responsive actuators based on graphene. *The Innovation*, **2021**, 2(4).
[29]. Panicker, S., Mohamed, A.A., Polymer nanocomposites for drug delivery applications. *Smart Polymer Nanocomposites*, **2023**, 461-472.
[30]. Kimura, Y., Haraguchi, K., Clay–alcohol–water dispersions: Anomalous viscosity changes due to network formation of clay nanosheets induced by alcohol clustering. *Langmuir*, **2017**, 33(19), 4758-4768.
[31]. Eom, Y., Kim, B.C., Solubility parameter-based analysis of polyacrylonitrile solutions in n, n-dimethyl formamide and dimethyl sulfoxide. *Polymer*, **2014**, 55(10), 2570-2577.
[32]. Ray, S.S., Okamoto, M., Polymer/layered silicate nanocomposites: A review from preparation to processing. *Progress in Polymer Science*, **2003**, 28(11), 1539-1641.
[33]. Min, H.S., Saha, D., Kalita, J., Sarma, M., Mukherjee, A., Ezekoye, B., Ezekoye, V.A., Sharma, A.K., Yewale, M.A., Baayramov, A., Nanostructure thin films: Synthesis and different applications. *Functionalized Nanomaterials I*, **2020**, 71-82.
[34]. Shen, Z., Simon, G.P., Cheng, Y.B., Comparison of solution intercalation and melt intercalation of polymer–clay nanocomposites. *Polymer*, **2002**, 43(15), 4251-4260.
[35]. Kumar, R., Singh, S., Yadav, B., Conducting polymers: Synthesis, properties and applications. *International Advanced Research Journal in Science, Engineering and Technology*, **2015**, 2(11), 110-124.
[36]. Parajuli, D., Mxenes-polymer nanocomposites for biomedical applications: Fundamentals and future perspectives. *Frontiers in Chemistry*, **2024**, 12, 1400375.
[37]. Gonçalves, R., Serra, J., Reizabal, A., Correia, D., Fernandes, L., Brito-Pereira, R., Lizundia, E., Costa, C., Lanceros-Méndez, S., Biobased polymers for

advanced applications: Towards a sustainable future. *Progress in Polymer Science*, **2025**, 101934.
[38]. Mahmood, N., Zhang, C., Yin, H., Hou, Y., Graphene-based nanocomposites for energy storage and conversion in lithium batteries, supercapacitors and fuel cells. *Journal of Materials Chemistry A*, **2014**, 2(1), 15-32.
[39]. Choy, J.H., Choi, S.J., Oh, J.M., Park, T., Clay minerals and layered double hydroxides for novel biological applications. *Applied Clay Science*, **2007**, 36(1-3), 122-132.
[40]. Ruiz-Hitzky, E., Darder, M., Fernandes, F.M., Wicklein, B., Alcântara, A.C., Aranda, P., Fibrous clays based bionanocomposites. *Progress in Polymer Science*, **2013**, 38(10-11), 1392-1414.
[41]. Spitalsky, Z., Tasis, D., Papagelis, K., Galiotis, C., Carbon nanotube–polymer composites: Chemistry, processing, mechanical and electrical properties. *Progress in Polymer Science*, **2010**, 35(3), 357-401.
[42]. Mondal, S.K., Prasad, K.R., Munichandraiah, N., Analysis of electrochemical impedance of polyaniline films prepared by galvanostatic, potentiostatic and potentiodynamic methods. *Synthetic Metals*, **2005**, 148(3), 275-286.
[43]. Vargas, P.C., Merlini, C., Ramôa, S.D.A.d.S., Arenhart, R., Barra, G.M.d.O., Soares, B.G., Conductive composites based on polyurethane and nanostructured conductive filler of montmorillonite/polypyrrole for electromagnetic shielding applications. *Materials Research*, **2018**, 21(5), e20180014.
[44]. Navarchian, A.H., Joulazadeh, M., Karimi, F., Investigation of corrosion protection performance of epoxy coatings modified by polyaniline/clay nanocomposites on steel surfaces. *Progress in Organic Coatings*, **2014**, 77(2), 347-353.
[45]. Ime, E.P., Ajor, E.J., Ekpan, F.M., Samuel, H.S., Egwuatu, O.P., Electrical Applications of Clay-Reinforced Recycled Plastic Composites. *Eurasian Journal of Science and Technology*, **2024**, 4(3), 165-178.
[46]. Madejová, J., Ftir techniques in clay mineral studies. *Vibrational Spectroscopy*, **2003**, 31(1), 1-10.
[47]. Farmer, V.C., The infrared spectra of minerals. **1974**, 4.
[48]. MacDiarmid, A., Chiang, J., Richter, A., Epstein, A.J., Polyaniline: A new concept in conducting polymers. *Synthetic Metals*, **1987**, 18(1-3), 285-290.
[49]. Frost, R.L., Kloprogge, J.T., Vibrational spectroscopy of ferruginous smectite and nontronite. *Spectrochimica Acta Part A: Molecular and Biomolecular Spectroscopy*, **2000**, 56(11), 2177-2189.
[50]. Olaremi, S.O., Afuape, A.R., Oguayo, C.P., Edun, O.J., Ajoge, H.N., Anyasi, U.P., Oni-Adimabua, O.N., Ukwesan, G.T., Oyinlade, P.O., Ibrahim, T.C., Ayeni, L.A., Oguadinma, C.O., Hayatu, S.J., Akintunde, M.O., Olokor, A.N., Afolabi, O.S., Effective removal of crystal violet dye from aqueous solutions using Periwinkle-clay rooftile composite catalyst: Experimental investigation and kinetic modelling, *Progress in Chemical and Biochemical Research*, **2024**, 7(4), 378-393.
[51]. Stejskal, J., Gilbert, R., Polyaniline. Preparation of a conducting polymer (iupac technical report). *Pure and Applied Chemistry*, **2002**, 74(5), 857-867.
[52]. Lefrant, S., Baibarac, M., Baltog, I., Raman and ftir spectroscopy as valuable tools for the characterization of polymer and carbon nanotube-based composites. *Journal of Materials Chemistry*, **2009**, 19(32), 5690-5704.
[53]. Drury, A., Chaure, S., Kröll, M., Nicolosi, V., Chaure, N., Blau, W.J., Fabrication and characterization of silver/polyaniline composite nanowires in porous anodic alumina. *Chemistry of Materials*, **2007**, 19(17), 4252-4258.
[54]. Farshi Azhar, F., Olad, A., Mirmohseni, A., Development of novel hybrid nanocomposites based on natural biodegradable polymer–montmorillonite/polyaniline: Preparation and characterization. *Polymer Bulletin*, **2014**, 71(7), 1591-1610.
[55]. Upadhyaya. M., Polyaniline/Clay nanocomposites-synthesis and characterization. *International Journal of Trend in Scientific Research and Development (IJTSRD)* **2022**, *6* (4), 357–368.
[56]. Soonmin, H., Thin film studies by energy dispersive x-ray analysis technique. *New Frontiers in Physical Science Research Vol. 5*, **2022**, 18-32.
[57]. Jiang, T., Kuila, T., Kim, N.H., Ku, B.C., Lee, J.H., Enhanced mechanical properties of silanized silica nanoparticle attached graphene oxide/epoxy composites. *Composites Science and Technology*, **2013**, 79, 115-125.
[58]. Ates, M., A review on conducting polymer coatings for corrosion protection. *Journal of Adhesion Science and Technology*, **2016**, 30(14), 1510-1536.
[59]. Sengupta, R., Bhattacharya, M., Bandyopadhyay, S., Bhowmick, A.K., A review on the mechanical and electrical properties of graphite and modified graphite reinforced polymer composites. *Progress in Polymer Science*, **2011**, 36(5), 638-670.
[60]. Para, M.L., Versaci, D., Amici, J., Caballero, M.F., Cozzarin, M.V., Francia, C., Bodoardo, S., Gamba, M., Synthesis and characterization of montmorillonite/polyaniline composites and its

usage to modify a commercial separator. *Journal of Electroanalytical Chemistry*, **2021**, 880, 114876.
[61]. Wu, Y.B., Mo, Z.L., Chen, H., Niu, G.P., Synthesis and characterization of polyaniline/montmorillonite/la^{3+} nanocomposites. *Advanced Materials Research*, **2009**, 79, 1547-1550.
[62]. Stejskal, J., Trchová, M., Bober, P., Humpolíček, P., Kašpárková, V., Sapurina, I., Shishov, M.A., Varga, M., Conducting polymers: Polyaniline. *Encyclopedia of Polymer Science and Technology*, **2002**, 1-44.
[63]. Julius, A., Malakondaiah, S., Pothireddy, R.B., Polymer and nanocomposite fillers as advanced materials in biomedical applications. *Nano Trends*, **2025**, 100087.
[64]. Babakhani, D., Hamidi, M., Possible application of ternary polyaniline-graphene-montmorillonite nanocomposite for electromagnetic pollution shielding. *Iranian Journal of Chemistry and Chemical Engineerig (IJCCE) Research,* **2024**, 43(2), 582-593.
[65]. Min, H.S., Scanning electron microscopy analysis of thin films: A review. *Research Aspects in Chemical and Materials Sciences*, **2022**, 5, 16-28.
[66]. Li, S., Meng Lin, M., Toprak, M.S., Kim, D.K., Muhammed, M., Nanocomposites of polymer and inorganic nanoparticles for optical and magnetic applications. *Nano Reviews*, **2010**, 1(1), 5214.
[67]. Abbas, M., Hachemaoui, A., Yahiaoui, A., Mourad, A.H.I., Belfedal, A., Cherupurakal, N., Chemical synthesis of nanocomposites via in-situ polymerization of aniline and iodoaniline using exchanged montmorillonite. *Polymers and Polymer Composites*, **2021**, 29(7), 982-991.
[68]. Kumar, A., Kumar, V., Awasthi, K., Polyaniline–carbon nanotube composites: Preparation methods, properties, and applications. *Polymer-Plastics Technology and Engineering*, **2018**, 57(2), 70-97.
[69]. Omastová, M., Trchová, M., Kovářová, J., Stejskal, J., Synthesis and structural study of polypyrroles prepared in the presence of surfactants. *Synthetic Metals*, **2003**, 138(3), 447-455.
[70]. Ray, S.S., Bousmina, M., Maazouz, A., Morphology and properties of organoclay modified polycarbonate/poly (methyl methacrylate) blend. *Polymer Engineering & Science*, **2006**, 46(8), 1121-1129.
[71]. Meneghetti, P., Qutubuddin, S., Synthesis, thermal properties and applications of polymer-clay nanocomposites. *Thermochimica Acta*, **2006**, 442(1-2), 74-77.
[72]. Trchová, M., Stejskal, J., Polyaniline: The infrared spectroscopy of conducting polymer nanotubes (iupac technical report). *Pure and Applied Chemistry*, **2011**, 83(10), 1803-1817.
[73]. Kibanova, D., Cervini-Silva, J., Destaillats, H., Efficiency of clay– TiO_2 nanocomposites on the photocatalytic elimination of a model hydrophobic air pollutant. *Environmental Science & Technology*, **2009**, 43(5), 1500-1506.
[74]. Lasia, A., Electrochemical impedance spectroscopy and its applications. *Modern Aspects of Electrochemistry*, **2002**, 143-248.
[75]. Ma, Y., Yue, Y., Zhang, H., Cheng, F., Zhao, W., Rao, J., Luo, S., Wang, J., Jiang, X., Liu, Z., 3d synergistical mxene/reduced graphene oxide aerogel for a piezoresistive sensor. *ACS Nano*, **2018**, 12(4), 3209-3216.
[76]. Saini, P., Choudhary, V., Singh, B., Mathur, R., Dhawan, S., Polyaniline–mwcnt nanocomposites for microwave absorption and emi shielding. *Materials Chemistry and Physics*, **2009**, 113(2-3), 919-926.
[77]. Al-Ghamdi, A., Al-Hartomy, O.A., Al-Solamy, F., Al-Hazmi, F., Al-Ghamdi, A.A., El-Mossalamy, E., El-Tantawy, F., On the prospects of conducting polyaniline/natural rubber composites for electromagnetic shielding effectiveness applications. *Journal of Thermoplastic Composite Materials*, **2014**, 27(6), 765-782.
[78]. Ho, S.M., Mariyappan, S., Meet, M., Jaysukh, H.M., Review on dye-sensitized solar cells based on polymer electrolytes. *International Journal of Engineering & Technology*, **2018**, 3001-3006.
[79]. Sood, Y., Singh, K., Mudila, H., Lokhande, P., Singh, L., Kumar, D., Kumar, A., Mubarak, N.M., Dehghani, M.H., Insights into properties, synthesis and emerging applications of polypyrrole-based composites, and future prospective: A review. *Heliyon*, **2024**, 10(13).
[80]. Mapossa, A.B., da Silva Júnior, A.H., De Oliveira, C.R.S., Mhike, W., Thermal, morphological and mechanical properties of multifunctional composites based on biodegradable polymers/bentonite clay: A review. *Polymers*, **2023**, 15(16), 3443.